

# Outcomes and Insights from Simplified Analytic Trajectory Optimization for a Tethered Underwater Kite

Miguel Alvarez\* and Hosam K. Fathy\*\*

**Abstract**—This paper formulates and solves a periodic trajectory optimization problem for a tethered underwater kite. The goal is to maximize the average mechanical power harvested by the kite. The type of kite considered in this work extracts electricity from ocean currents by moving cross-current as its reel away from its base station, and consumes electricity to reel back. The problem of optimizing this kite’s trajectory is challenging due to the high dimensionality and nonlinearity of its dynamics. To tackle this challenge, the literature often separates the problem into two subproblems focusing on optimizing the cross-current and the reel-in/reel-out components of the trajectory, respectively, which may be sub-optimal. In contrast, this work solves for the combined cross-current and reel-in/reel-out trajectory by linearizing the dynamics of the kite around a zero-power reference equilibrium trajectory in spherical coordinates. This allows the trajectory optimization problem to be solved analytically for simple sinusoidal input perturbations from equilibrium. We use linear quadratic regulation to enable the nonlinear kite model to track the optimized trajectory. The result is a computationally efficient approach that achieves an attractive Loyd factor of 19.9%, while providing important insights into the nature of the optimal trajectory.

**Index Terms**—Energy systems; optimization.

## I. INTRODUCTION

THIS paper optimizes the periodic trajectory of a kite that harvests energy from ocean currents: a relatively unexploited green resource. Fast ocean currents include western boundary currents (WBC), which flow in the western regions of oceans along continental shores. These WBCs have a typical width of 100 km and height of 1000 m with speeds that can reach  $3 \text{ m s}^{-1}$  [1]. One example is the Gulf Stream, where measurements near the North Carolina shore at a depth of 75 m yielded a mean water speed of  $1.07 \text{ m s}^{-1}$  for an entire year of measurements [1]. We can estimate the power density of the water as:

$$P = \frac{1}{2} \rho v^3 \quad (1)$$

where,  $P$ ,  $\rho$  and  $v$  are the power density in  $\text{W m}^{-2}$ , the density of water, and the speed of the fluid, respectively. This suggests

that the Gulf Stream at that location has an average power density of  $1000 \text{ W m}^{-2}$ .

Multiple marine hydrokinetic (MHK) systems have been proposed to extract energy from the above currents, including kites [2]–[4]. The evolution of these kites was initially inspired by tethered airborne wind energy systems (AWES) [5], largely motivated by seminal research by Loyd [6]. Both MHK and AWES kites can fly cross-current to amplify the apparent kite speed relative to the surrounding fluid. They generate electricity either with an on-board generator, or by reeling out a tether attached to a generator in a stationary platform. The latter “pumping” configuration is the focus of this work.

Tethered kites rely on active control to generate energy. Typically, the kite trajectory consists of a high tension regime as the kite is reeled out, and a low tension regime as it is reeled in. Given the importance of control in the energy generation potential of MHK systems, significant research focuses on the design of these controllers. One challenge the literature addresses is trajectory optimization for these systems. Naturally, the overall objective is to maximize the net power generation of the system. Because of the complexity of the resulting optimization problem, researchers typically simplify this problem prior to solving it. One possible simplification is to optimize the kite’s reel-in/reel-out and cross-current trajectories either independently or sequentially. Another simplification is to divide the problem into a power generation phase and a power consumption phase, then perform optimization separately for each phase. A third possibility is to simplify the objective by maximizing a proxy for generated power, such as tension force [7], [8]. Other work in the AWES literature simplifies the optimization problem by pre-imposing a topological constraint on the kite path, such as forcing it to navigate in figure-8 shapes. Optimization then proceeds using tools such as direct transcription [9], [10]. Part of the literature on controlling the kite focuses on adaptive schemes to solve the trajectory generation problem. These schemes include: robust and passivity-based control [11], [12], extremum seeking [13], Bayesian optimization [14], [15], iterative learning [16], and maximum power point tracking [17].

The main goal in this paper is to simultaneously optimize the reel-in/reel-out and cross-current trajectories of an energy-harvesting kite. The paper’s novelty stems from its use of a new simplification approach to both achieve attractive net power generation levels and yield important insights into the underlying optimization problem. Specifically, we use a 3DOF

\* Ph.D. student (malvarez@umd.edu), \*\* professor and corresponding author (hfathy@umd.edu), Mechanical Engineering Department, The University of Maryland, College Park. The research in this paper was funded by a Marine Hydrokinetics research grant from the Department of Energy’s EERE Office. The authors gratefully acknowledge this support.

model of the kite in spherical coordinates and linearize it around a zero-power circular cross-current equilibrium trajectory. This makes it possible to formulate power maximization as a simple indefinite quadratic optimal control problem with linear dynamic constraints. Expressing the kite's input trajectory in terms of sinusoidal perturbations from equilibrium makes it possible to translate this problem into an even simpler static indefinite quadratic problem. We use traditional linear quadratic regulation to force the nonlinear kite dynamics to track the solution to this linearized problem. This approach furnishes a very attractive net power generation level, considering its simplicity, with a Loyd factor approaching 20%. Moreover, the approach yields important insights into the nature of the optimal trajectory, one example being the degree to which reel-out and reel-in are achieved in the plane perpendicular to the free-stream flow. The remainder of the paper: presents the kite model; formulates and solves the kite trajectory optimization problem; then finally simulates the non-linear kite model and examines its performance as it tracks the trajectory generated by the simplified linear analysis.

## II. KITE MODEL

This section proposes a simplified 3-degree-of-freedom model of the kite. The model assumes that the kite's attitude dynamics (roll, pitch, and yaw) can be controlled by lower-level controllers to track a desired attitude trajectory accurately. This allows the higher-level optimization work in this paper to focus on the translational dynamics of the kite, represented as a point mass. In solving this optimization problem, we treat the rates of change of the kite's angle of attack, induced roll (or banking) angle, and tether tension as control inputs that can be manipulated to achieve a desired translation trajectory. Additionally, we assume that the kite is neutrally buoyant, meaning that its weight cancels with the buoyancy force. Perhaps most importantly, we examine the special case where the kite's anchor point is immersed underwater at a sufficient depth to allow the kite to fly in a circular, zero-power cross-current equilibrium trajectory centered directly downstream of this anchor point. We use this reference trajectory as a starting point for linearizing the kite's dynamics. This assumption places some limitations on the kite's anchoring system, but makes it possible to obtain important analytic insights into the nature of the optimal kite trajectory.

The kite's underwater motion is governed by the forces acting on it, namely, the: gravitational, tension, buoyancy, and hydrodynamic surface forces. The hydrodynamic surface forces are typically decomposed into lift, drag, and side force. We define a spherical coordinate frame  $\mathcal{S}$  with unit vectors:  $\{\hat{e}_r, \hat{e}_\theta, \hat{e}_\psi\}$ . We can relate this frame to a Cartesian frame as shown in Figure 1. We can write the position vector and its derivatives:

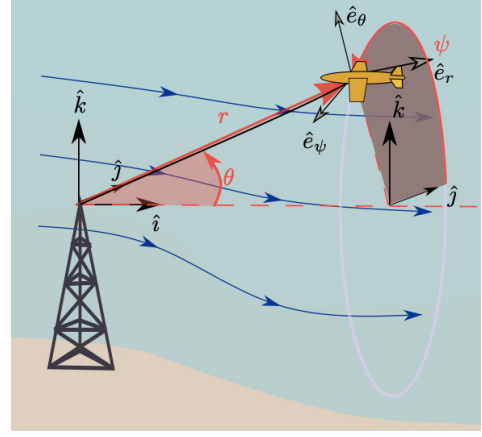


Fig. 1. Underwater kite with unit vectors in Cartesian and spherical coordinates

$$\mathbf{r} = r\hat{e}_r \quad (2)$$

$$\dot{\mathbf{r}} = \dot{r}\hat{e}_r + r\dot{\theta}\hat{e}_\theta + r\dot{\psi}\sin\theta\hat{e}_\psi \quad (3)$$

$$\begin{aligned} \ddot{\mathbf{r}} = & \left( \ddot{r} - r\dot{\theta}^2 - r\dot{\psi}^2\sin\theta\cos\theta \right) \hat{e}_r \\ & + \left( \dot{r}\dot{\theta} + r\ddot{\theta} - r\dot{\psi}^2\sin\theta \right) \hat{e}_\theta \\ & + \left( \dot{r}\dot{\psi}\sin\theta + r\ddot{\psi}\sin\theta + r\dot{\psi}\dot{\theta}\cos\theta \right) \hat{e}_\psi \end{aligned} \quad (4)$$

We can now write an expression for the relative velocity of the kite with respect to the fluid. We define the velocity of the water along the  $\hat{i}$  direction:  $\mathbf{V}_w = u_w\hat{i}$ . In spherical coordinates this becomes  $\mathbf{V}_w = u_w\cos\theta\hat{e}_r - u_w\sin\theta\hat{e}_\theta$ . The relative velocity is thus:

$$\mathbf{V}_{rel} = \dot{\mathbf{r}} - \mathbf{V}_w \quad (5)$$

$$\mathbf{V}_{rel} = (\dot{r} - u_w\cos\theta)\hat{e}_r + (r\dot{\theta} + u_w\sin\theta)\hat{e}_\theta + r\dot{\psi}\sin\theta\hat{e}_\psi \quad (6)$$

Let us define a new frame  $\mathcal{W}$  with respect to which we will define the external forces applied to this kite.

$$\hat{x}_w = \frac{\mathbf{V}_{rel}}{|\mathbf{V}_{rel}|}, \quad \hat{z}_w = \frac{\hat{x}_w \times \mathbf{r}}{|\hat{x}_w \times \mathbf{r}|}, \quad \hat{y}_w = \frac{\hat{z}_w \times \hat{x}_w}{|\hat{z}_w \times \hat{x}_w|} \quad (7)$$

The forces the kite experiences are:

$$\mathbf{L} = \frac{1}{2}\rho SC_L(\alpha)|\mathbf{V}_{rel}|^2(\cos(\phi)\hat{y}_w + \sin(\phi)\hat{z}_w) \quad (8)$$

$$\mathbf{D} = -\frac{1}{2}\rho SC_D(\alpha)|\mathbf{V}_{rel}|^2\hat{x}_w \quad (9)$$

$$\mathbf{T} = T\frac{\mathbf{r}}{|\mathbf{r}|} \quad (10)$$

These are illustrated in Figure 2. where  $T, \alpha, \phi$  are the scalar tension force (always negative), the angle of attack, and the roll angle, respectively. The other parameters  $\rho, C_L, C_D$ , and  $S$  are, respectively, the water density, the lift coefficient, the drag

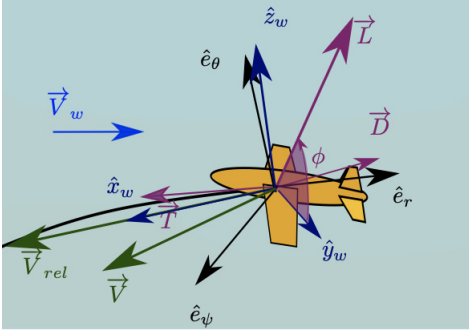


Fig. 2. Water frame and external forces

coefficient, and the wing area. The hydrodynamic coefficients  $C_L$  and  $C_D$  are modeled in terms of  $\alpha$  as follows:

$$C_L(\alpha) = c_1\alpha + c_2 \quad (11)$$

$$C_D(\alpha) = b_1\alpha^2 + b_2\alpha + b_3 \quad (12)$$

The equations of motion for this kite are thus given by:

$$m\ddot{\mathbf{r}} = \sum \mathbf{F}_{ext} \quad (13)$$

where  $\sum \mathbf{F}_{ext} = \mathbf{L} + \mathbf{D} + \mathbf{T}$ .

We express the above equations of motion in state-space form, with two important caveats. First, we note that in the absence of flow shear (i.e., if free-stream water velocity is spatially uniform), we do not need to include  $\psi$  as a state variable in the model. This makes it possible to represent a zero-power circular trajectory perpendicular to the free-stream flow as a single equilibrium point in the kite's state space. Our optimization study utilizes a dynamic model linearized around this equilibrium. Second, to ensure a smooth trajectory, our optimization problem penalizes the rates of change of the kite's angle of attack  $\alpha$ , induced roll angle  $\phi$ , and tension  $T$ . To allow for such a penalty within a standard optimal control problem formulation, we make the rates of change of these three state variables control inputs. This leads to a state-space model of the form below:

$$\frac{d}{dt}X = f(X, U) \quad (14)$$

where  $X = [r \ \theta \ v \ p \ q \ T \ \alpha \ \phi]^T$ ,  $U = [u_1 \ u_2 \ u_3]^T$ , and:

$$f(X, U) = \begin{bmatrix} v \\ p \\ \frac{\mathbf{F}}{m} \cdot \hat{e}_r + rp^2 + rq^2 \sin \theta \\ \frac{1}{r} \left( \frac{\mathbf{F}}{m} \cdot \hat{e}_\theta - vp + rq^2 \sin \theta \cos \theta \right) \\ \frac{1}{r \sin \theta} \left( \frac{\mathbf{F}}{m} \cdot \hat{e}_\psi - vq \sin \theta - rqp \cos \theta \right) \\ u_1 \\ u_2 \\ u_3 \end{bmatrix} \quad (15)$$

### III. PROBLEM FORMULATION

#### A. Optimization Objective

We formulate a periodic kite trajectory optimization problem with the following structure:

$$\text{Minimize } J = \int_0^T L(X, U) dt \quad (16)$$

$$\text{Subject to: } \dot{X} = f(X, U), X(0) = X(T) \quad (17)$$

The objective function in this problem is given by  $L(X, U) = -P + U^T R U$ , where  $P(t)$  is instantaneous mechanical power given by  $P = -vT$  and  $U^T R U$  is a positive-definite quadratic penalty on the control input vector. Thus, the optimization objective reflects a desire to maximize cycle-averaged mechanical power with a penalty on the rates of change of the physical control inputs needed for doing so. The mechanical power term is positive when the kite harvests energy and negative when it is reeled in. Note that this power term can be written in quadratic form as  $P = X^T Q X$ , where the state vector  $X$  contains the kite velocity  $v$  and tether tension  $T$ , implying that the matrix  $Q$  is negative semi-definite. Therefore, the above optimization problem has a non-convex quadratic objective.

#### B. Model Linearization

Solving the above trajectory optimization problem is difficult due to its nonlinearity, non-convexity, and high dimensionality (with 8 state variables). The problem becomes much simpler if one solves it approximately in the neighborhood of a state-input pair,  $X_{eq}, U_{eq}$ , satisfying the definition of an equilibrium point, i.e.,

$$f(X_{eq}, U_{eq}) = \mathbf{0} \quad (18)$$

The kite has an infinite number of equilibria, corresponding to different circular trajectories in a plane perpendicular to the free-stream water velocity vector, with the centers of the circles aligned with the tether anchor point. For any given equilibrium, the kite's dynamics can be linearized to furnish:

$$\frac{d}{dt}\tilde{X} = A\tilde{X} + B\tilde{U} \quad (19)$$

where  $\tilde{X}$  and  $\tilde{U}$  represent state/input perturbations from equilibrium,  $A = [\partial f / \partial X]_{eq}$ , and  $B = [\partial f / \partial U]_{eq}$

#### C. Simplified Optimization Problem

Linearizing the dynamics of the kite around a reference equilibrium simplifies the above trajectory optimization problem significantly as follows:

$$\text{Minimize } J = \int_0^T L(X_{eq} + \tilde{X}, U_{eq} + \tilde{U}) dt \quad (20)$$

$$\text{Subject to: } \dot{\tilde{X}} = A\tilde{X} + B\tilde{U}, \tilde{X}(0) = \tilde{X}(T) \quad (21)$$

The above problem can be simplified further as follows. First, recall that the input vector  $U(t)$  consists of the rates of

change of the kite's angle of attack, roll angle, and tether tension. All three of these state variables are constant at equilibrium, meaning that the equilibrium input  $U_{eq}$  must equal zero. As a result,  $U(t) = U_{eq} + \tilde{U}(t)$  must equal  $\tilde{U}(t)$  and therefore the control input penalty simplifies to  $\tilde{U}^T R \tilde{U}$ . Second, since the tether release rate  $v(t)$  must equal zero at equilibrium, one can conclude that  $v(t) = v_{eq} + \tilde{v}(t)$  must equal  $\tilde{v}(t)$ . By definition, mechanical power is given by  $P(t) = v(t)T(t) = (v_{eq} + \tilde{v}(t))(T_{eq} + \tilde{T}(t))$ , a term that simplifies to  $\tilde{v}(t)(T_{eq} + \tilde{T}(t))$ . Furthermore, expressing the optimal periodic trajectory of  $\tilde{v}(t)$  as a Fourier series leads to the conclusion that the cycle average of  $\tilde{v}(t)T_{eq}$  is zero. Combining all of these insights leads to the following simplified trajectory optimization problem statement:

$$\text{Min. } J = \int_0^T L(\tilde{X}, \tilde{U}) dt = \int_0^T \tilde{X}^T Q \tilde{X} + \tilde{U}^T R \tilde{U} dt \quad (22)$$

$$\text{Subject to: } \dot{\tilde{X}} = A\tilde{X} + B\tilde{U}, \tilde{X}(0) = \tilde{X}(T) \quad (23)$$

#### D. Analytical Solution

The above simplified trajectory optimization problem has linear dynamics and a non-convex objective, thanks to the fact that the matrix  $Q$  is negative semi-definite. As a result, this problem's solution is unbounded in terms of the magnitudes of the optimal state and input perturbations  $\tilde{X}$  and  $\tilde{U}$ , respectively. In practice, the optimal kite trajectory is bounded by space constraints as well as the diminishing accuracy of the above linearized kite model for larger motion magnitudes. With this in mind, we analyze the structure of the problem for a sinusoidal input trajectory of the form:

$$\tilde{U}(t) = \mathbf{u}_1 \sin \omega t + \mathbf{u}_2 \cos \omega t \quad (24)$$

where  $\omega$  is the frequency of the sinusoidal trajectory, and the coefficients  $\mathbf{u}_1$  and  $\mathbf{u}_2$  are assumed to be small. With a sinusoidal input trajectory and linear dynamics we can analytically obtain an expression for the state variables as a function of time. The linear dynamics of the system are represented by the transfer function of the system  $G(s)$  in the Laplace domain.

$$G(s) = [sI - A]^{-1} B \quad (25)$$

We can now write an analytical expression for our state variables as a function of time as follows:

$$\tilde{X}(t) = (G_r \mathbf{u}_1 - G_i \mathbf{u}_2) \sin \omega t + (G_i \mathbf{u}_1 + G_r \mathbf{u}_2) \cos \omega t \quad (26)$$

where  $G_r$  and  $G_i$  are the real and imaginary components of  $G(s)|_{s=j\omega}$ . Notice that the transfer function enforces the dynamic constraint in our linearized optimization problem. Moreover, the focus on the steady-state response to a sinusoidal input trajectory ensures periodicity.

We can substitute expressions (24) and (26) into the objective (20) and obtain a static optimization problem where the optimization variables are the vectors  $\mathbf{u}_1$  and  $\mathbf{u}_2$ . We

can thus re-write the optimization problem. After linearizing the dynamics of the system and imposing a sinusoidal input trajectory our optimization problem becomes an unconstrained static quadratic optimization problem.

$$\text{Minimize } J = \frac{\pi}{2\omega} [\mathbf{u}_1 \quad \mathbf{u}_2] \Phi_{6 \times 6} \begin{bmatrix} \mathbf{u}_1 \\ \mathbf{u}_2 \end{bmatrix} \quad (27)$$

where

$$\Phi_{[1:3,1:3]} = \Phi_{[3:6,3:6]} = R + G_r^T Q G_r + G_i^T Q G_i \quad (28)$$

$$\Phi_{[1:3,3:6]} = \Phi_{[3:6,1:3]} = [0]_{3 \times 3} \quad (29)$$

The matrix  $\Phi$  is indefinite, suggesting that the solution to this problem is unbounded. To better understand the structure of this solution, we focus on the particular direction in the optimization space that yields the fastest decrease in the minimization objective. In other words, we focus on the eigenvector of the matrix  $\Phi$  associated with its most negative eigenvalue. Denoting this eigenvector by  $\mathbf{v}$ , we select:

$$\begin{bmatrix} \mathbf{u}_1 \\ \mathbf{u}_2 \end{bmatrix} = \lambda \mathbf{v} \quad (30)$$

where  $\lambda$  is a scaling gain. In the linearized optimization problem, increasing this gain to infinity always yields benefits, at the expense of increasing departure from the true nonlinear dynamics. This motivates the final step in our analysis, where we use linear quadratic regulation to enable the nonlinear kite dynamics to track the above optimal trajectory for different values of  $\lambda$ , thereby gaining insight into the practical limitations on the magnitude of  $\lambda$ .

## IV. RESULTS

### A. Performance Metric

To evaluate the performance of our control approach we can compare the average power the kites generate to the maximum theoretical power it can generate – namely, Loyd's limit. We will call the ratio of these quantities the Loyd factor. The Loyd limit [18] is defined as:

$$P = \frac{2}{27} \rho S u_w^3 C_L \left( \frac{C_L}{C_D} \right)^2 \quad (31)$$

### B. Kite Linear Quadratic Regulator

The state and input trajectories generated in the previous sections assume that the dynamics of the kite are linear. The further the kite's trajectory deviates from equilibrium, the less this assumption is valid. We propose to use the obtained trajectories as a reference to a linear-quadratic regulator. We then simulate the non-linear kite model as it attempts to track this reference.

We formulate the LQR problem as follows:

$$\text{Minimize } J = \int_0^\infty (X_{error}^T Q_{LQR} X_{error} + U^T R_{LQR} U) dt \quad (32)$$

$$\text{Subject to: } \dot{X}_{error} = A X_{error} + B U \quad (33)$$

This problem has a steady-state solution of the form:

$$U = -K_{LQR}X_{error} \quad (34)$$

The feedback gain matrix  $K_{LQR}$  will depend on  $Q_{LQR}$ ,  $R_{LQR}$ ,  $A$  and  $B$ .

### C. Numerical Simulation

To evaluate our control strategy we simulate a non-linear kite as it tracks the reference sinusoidal trajectory obtained in the previous section. To avoid large control inputs at initialization, we start the kite at equilibrium and gradually increase the magnitude of the reference trajectory. Table IV-C contains the parameters used for the simulation.

TABLE I  
PARAMETERS

| Kite Parameters           |                          |                        |                   |
|---------------------------|--------------------------|------------------------|-------------------|
| Mass                      | $m$                      | 2700                   | kg                |
| Wing reference area       | $S$                      | 10                     | m <sup>2</sup>    |
| Aerodynamic coefficients  | $c_1$                    | $6.25 \times 10^{-2}$  | deg <sup>-1</sup> |
|                           | $c_2$                    | $1.33 \times 10^{-1}$  | -                 |
|                           | $b_1$                    | $2.442 \times 10^{-4}$ | deg <sup>-2</sup> |
|                           | $b_2$                    | $1.06 \times 10^{-3}$  | deg <sup>-1</sup> |
|                           | $b_3$                    | $2.22 \times 10^{-3}$  | -                 |
| Flow Parameters           |                          |                        |                   |
| Water density             | $\rho$                   | 1000                   | kg/m <sup>3</sup> |
| Water speed               | $u_w$                    | 1                      | m/s               |
| Optimization Parameters   |                          |                        |                   |
| Input quadratic penalties | $R_{11}$                 | 0                      | -                 |
|                           | $R_{22}$                 | $10 \times 10^9$       | -                 |
|                           | $R_{33}$                 | $30 \times 10^9$       | -                 |
| Controller Parameters     |                          |                        |                   |
|                           | $q_{11}, q_{22}, q_{33}$ | $2 \times 10^{12}$     | -                 |
|                           | $q_{44}$                 | $2 \times 10^{14}$     | -                 |
|                           | $q_{55}$                 | $2 \times 10^{13}$     | -                 |
|                           | $q_{66}, q_{77}$         | $2 \times 10^2$        | -                 |
|                           | $q_{88}$                 | $2 \times 10^{-1}$     | -                 |
|                           | $q_{99}$                 | $2 \times 10^{11}$     | -                 |
|                           | $r_{11}$                 | $1 \times 10^{-6}$     | -                 |
|                           | $r_{22}$                 | $1 \times 10^8$        | -                 |
|                           | $r_{33}$                 | $2 \times 10^{10}$     | -                 |

Figure 3 shows the position trajectory of the kite for the last 3 periods of simulation. One interesting feature of this result is that the kite reels away by mostly moving cross-current instead of parallel to the flow. In fact, the kite's downstream distance from the tether anchor point experiences relatively modest changes, with much of the reel-in and reel-out action occurring "in plane". One possible explanation is the degree to which the kite's fast cross-current motion makes such an oval in-plane trajectory both feasible and attractive. This is an important insight, and not necessarily an intuitive one compared a trajectory where reel-in and reel-out occur along the free-stream flow direction.

Figures 4 and 5 show the power, release rate, and tension trajectories for the linear and non-linear kite models. The

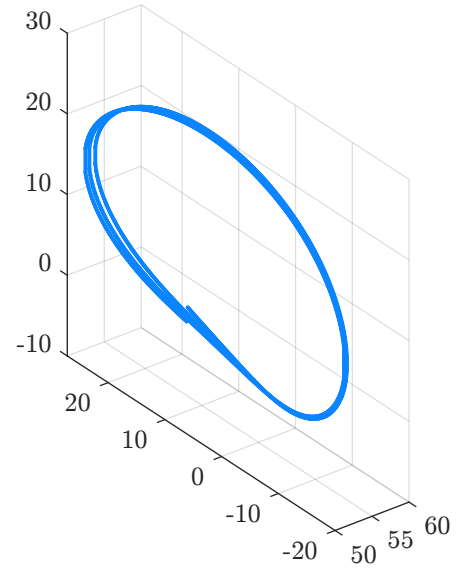


Fig. 3. Path of the non-linear kite model in the last 3 periods of simulation

average power of the non-linear kite for this simulation is 16.4kW which corresponds to Loyd factor of 19.9%. This is an attractive outcome, particularly in light of the simplicity of the approach used for achieving it.

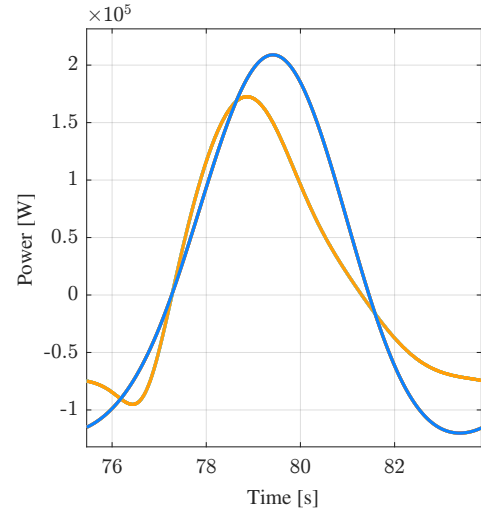


Fig. 4. Power generated in the last period of simulation. Orange line: Non-linear model, Blue line: Linear model.

### D. Sensitivity to eigenvector scaling

Finally we explore how changing the scaling factor  $\lambda$  affects the generated power in these simulations. For this, we keep all parameters equal and do a sweep on the scaling factor  $\lambda$ . Figure 6 shows the average power generated by the nonlinear model (vertical axis) versus the average power generated by the linear model (horizontal axis) as the scaling factor  $\lambda$  increases. The increasing scaling factor corresponds to larger deviations from equilibrium and the power generated by the non-linear model decreases in comparison to the linear one for increasing deviations. This places a practical limit on how

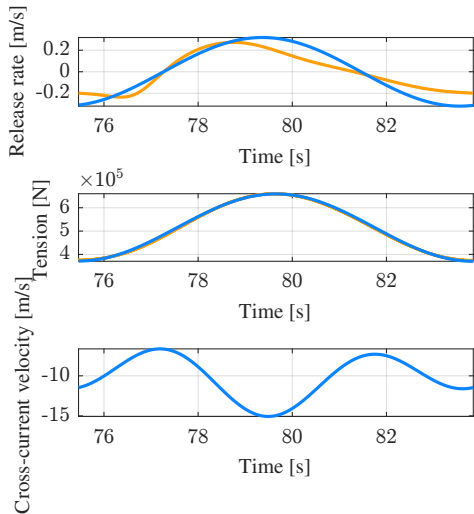


Fig. 5. Release rate, tension and cross-current velocity for the last period of simulation. Orange: Non-linear model, Blue: Linear model.

far one can “push” the solution of this optimization problem, even if the underlying simplified linear analysis leads to an unbounded solution.

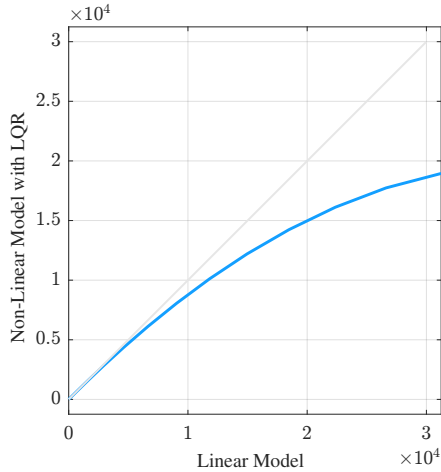


Fig. 6. Average power generated by non-linear model vs. average power generated by linear model as the scaling factor  $\lambda$  increases

## V. CONCLUSION

In this paper we proposed to maximize the power generated by an underwater kite that operates in pumping mode. For this we derive a simplified 3DOF nonlinear kite model and formulate an optimization problem to maximize the mechanical power of the kite while minimizing the inputs. By performing simplifications such as linearizing the kite model and imposing a sinusoidal input trajectory we are able to transform a dynamic quadratic optimization problem into an unconstrained static optimization problem. We use the objective of this problem to obtain trajectories along its steepest direction of descent. By introducing a scaling factor we are able to adjust how much we deviate from the equilibrium of the system. The resulting trajectories were then tracked by a non-linear kite

with a linear quadratic regulator. For a  $1\text{m s}^{-1}$  flow speed and a kite with a wing area of  $10\text{m}^2$  we generated an average power of  $16.4\text{kW}$  corresponding to a Loyd factor of  $19.9\%$ . An increase in the scaling factor increases the generated power with decreasing gains as the trajectories depart further from equilibrium.

## REFERENCES

- [1] J. M. Bane, R. He, M. Muglia, C. F. Lowcher, Y. Gong, and S. M. Haines, “Marine hydrokinetic energy from western boundary currents,” *Annual Review of Marine Science*, vol. 9, no. 1, pp. 105–123, jan 2017.
- [2] D. J. Olinger and Y. Wang, “Hydrokinetic energy harvesting using tethered undersea kites,” *Journal of Renewable and Sustainable Energy*, vol. 7, no. 4, p. 043114, July 2015.
- [3] C. Vermillion, M. Cobb, L. Fagiano, R. Leuthold, M. Diehl, R. S. Smith, T. A. Wood, S. Rapp, R. Schmehl, D. Olinger, and M. Demetriou, “Electricity in the air: Insights from two decades of advanced control research and experimental flight testing of airborne wind energy systems,” *Annual Reviews in Control*, apr 2021.
- [4] M. Landberg, “Submersible plant,” Aug. 21 2012, uS Patent 8,246,293.
- [5] C. Vermillion and L. Fagiano, “Electricity in the air: Tethered wind energy systems,” *Mechanical Engineering*, vol. 135, no. 09, pp. S13–S21, 2013.
- [6] M. L. Loyd, “Crosswind kite power (for large-scale wind power production),” *Journal of Energy*, vol. 4, no. 3, pp. 106–111, may 1980.
- [7] A. U. Zraggen, L. Fagiano, and M. Morari, “On real-time optimization of airborne wind energy generators,” in *52nd IEEE Conference on Decision and Control*. IEEE, 2013, pp. 385–390.
- [8] A. U. Zraggen, L. Fagiano, and M. Morari, “Real-time optimization and adaptation of the crosswind flight of tethered wings for airborne wind energy,” *IEEE Transactions on Control Systems Technology*, vol. 23, no. 2, pp. 434–448, 2015.
- [9] M. Erhard, G. Horn, and M. Diehl, “A quaternion-based model for optimal control of an airborne wind energy system,” *ZAMM - Journal of Applied Mathematics and Mechanics / Zeitschrift für Angewandte Mathematik und Mechanik*, vol. 97, no. 1, pp. 7–24, 2017.
- [10] J. Stuyts, G. Horn, W. Vandermeulen, J. Driesen, and M. Diehl, “Effect of the electrical energy conversion on optimal cycles for pumping airborne wind energy,” *IEEE Transactions on Sustainable Energy*, vol. 6, no. 1, pp. 2–10, jan 2015.
- [11] J. Alvarez-Gallegos, R. Castro-Linares, and M. Zempoalteca-Jimenez, “Robust nonlinear flight control of a power-generating tethered kite,” in *2019 16th International Conference on Electrical Engineering, Computing Science and Automatic Control (CCE)*. IEEE, 2019, pp. 1–6.
- [12] H. Li, D. J. Olinger, and M. A. Demetriou, “Passivity based control of a tethered undersea kite energy system,” in *2016 American Control Conference (ACC)*, 2016, pp. 4984–4989.
- [13] M. Kehs, C. Vermillion, and H. Fathy, “Online energy maximization of an airborne wind energy turbine in simulated periodic flight,” *IEEE Transactions on Control Systems Technology*, vol. 26, no. 2, pp. 393–403, 2018.
- [14] A. Baheri and C. Vermillion, “Waypoint optimization using bayesian optimization: A case study in airborne wind energy systems,” in *2020 American Control Conference (ACC)*. IEEE, 2020, pp. 5102–5017.
- [15] J. Deese and C. Vermillion, “Recursive Gaussian Process-Based Adaptive Control, With Application to a Lighter-Than-Air Wind Energy System,” *IEEE Transactions on Control Systems Technology*, pp. 1–8, 2020.
- [16] M. K. Cobb, K. Barton, H. Fathy, and C. Vermillion, “Iterative learning-based path optimization for repetitive path planning, with application to 3-d crosswind flight of airborne wind energy systems,” *IEEE Transactions on Control Systems Technology*, vol. 28, no. 4, pp. 1447–1459, 2020.
- [17] G. Mademlis, Y. Liu, P. Chen, and E. Singhroy, “Design of maximum power point tracking for dynamic power response of tidal undersea kite systems,” *IEEE Transactions on Industry Applications*, vol. 56, no. 2, pp. 2048–2060, 2020.
- [18] M. Diehl, “Airborne wind energy: Basic concepts and physical foundations,” Berlin, Heidelberg, pp. 3–22, 2013.